ESC HEART FAILURE
ESC Heart Failure 2021; **8**: 2310–2315
Published online 9 April 2021 in Wiley Online Library (wileyonlinelibrary.com) **DOI:** 10.1002/ehf2.13260

CASE REPORT

Novel dilated cardiomyopathy associated to *Calreticulin* and *Myo7A* gene mutation in Usher syndrome

Andrea Frustaci[1,4]*, Alessandro De Luca[2], Nicola Galea[3], Romina Verardo[4], Valentina Guida[2], Rosalba Carrozzo[5], Cristina Chimenti[1,4], Emanuela Frustaci[4], Luigi Sansone[6] and Matteo Antonio Russo[7]

[1]*Department of Clinical, Internal, Anesthesiologist and Cardiovascular Sciences, Sapienza University, Viale del Policlinico 155, Rome, 00161, Italy;* [2]*Medical Genetics Division, Fondazione IRCSS Casa Sollievo della Sofferenza, San Giovanni Rotondo, Italy;* [3]*Department of Experimental Medicine, Sapienza University, Rome, Italy;* [4]*Cellular and Molecular Cardiology Lab, IRCCS L. Spallanzani, Rome, Italy;* [5]*Molecular Medicine Laboratory, Department of Neuroscience and Neurorehabilitation, IRCCS Bambino Gesù Pediatric Hospital, Rome, Italy;* [6]*Laboratory of Molecular and Cellular Pathology, IRCCS San Raffaele Pisana, Rome, Italy;* [7]*MEBIC Consortium, San Raffaele Open University and IRCCS San Raffaele Pisana, Rome, Italy*

Abstract

We report a novel cardiomyopathy associated to Usher syndrome and related to combined mutation of *MYO7A* and *Calreticulin* genes. A 37-year-old man with deafness and vision impairment because of retinitis pigmentosa since childhood and a *MYO7A* gene mutation suggesting Usher syndrome, developed a dilated cardiomyopathy with ventricular tachyarrhythmias and recurrent syncope. At magnetic resonance cardiomyopathy was characterized by left ventricular dilatation with hypo-contractility and mitral prolapse with valve regurgitation. At left ventricular endomyocardial biopsy, it was documented cardiomyocyte disconnection because of cytoskeletal disorganization of cell-to-cell contacts, including intercalated discs, and mitochondrial damage and dysfunction with significant reduction of adenosine triphosphate production in patient cultured fibroblasts. At an extensive analysis by next-generation-sequencing of 4183 genes potentially related to the cardiomyopathy a pathogenic mutation of calreticulin was found. The cardiomyopathy appeared to be functionally and electrically stabilized by a combination therapy including carvedilol and amiodarone at a follow-up of 18 months.

Keywords Usher syndrome; *MYO7A*; *CALR*; Calreticulin; Cardiomyocyte disconnection

Received: 4 December 2020; Revised: 1 February 2021; Accepted: 6 February 2021
**Correspondence to: Andrea Frustaci, Department of Clinical, Internal, Anesthesiologist and Cardiovascular Sciences, Sapienza University, Viale del Policlinico 155, 00161, Rome, Italy. Tel: + 39 06 5517 0520. Email: biocard@inmi.it*

Introduction

Usher syndrome (US) is a rare,[1] congenital, and genetically heterogeneous entity characterized by deafness and vision loss. *MYO7A* (MIM# 276903) mutations with loss of function are most frequently observed for this syndrome and categorize its Type 1 (MIM# 276900).[2,3]

Here, we have studied a US patient bearing a classical *MYO7A* mutation and a mutation of calreticulin (*CALR*; MIM# 109091) gene, associated to a novel dilated cardiomyopathy.

Case report

A 37-year-old man with deafness and vision impairment because of retinitis pigmentosa since childhood and a *MYO7A* gene mutation denoting Type 1 US, was admitted because of recurrent syncope. Blood pressure was normal, and physical examination was unremarkable except for irregular heart rhythm. ECG showed sinus rhythm 80 bts/min and frequent ventricular extrasystoles with right bundle branch block configuration often in ventricular bigeminism. At Holter monitoring 15 280 ventricular ectopic beats were registered in 24 h

including couples, triplets, and short phases of non-sustained ventricular tachycardia.

Cardiac magnetic resonance (CMR) images showed a mildly dilated left ventricle (End diastolic volume [EDV]/Body surface area [BSA]: 105 mL/m^2) with normal thickness of ventricular wall (*Figure 1A,B*), and moderate reduction of systolic function (EF: 42%, *Figure 1C*).

Interestingly, the patient presented systolic mitral-annular disjunction with mitral valve prolapsed and moderate valve regurgitation (see arrow, *Figure 1D,E*). Mitral annular disjunction occurred with hypotonia of posterior papillary muscle and abnormal stretching of the cords (Supporting information, *Movies S1* and *S2*) suggesting contractile impairment. No areas of myocardial fibrosis were detected at late gadolinium enhanced imaging (*Figure 1F,G*). No CMR criteria for left ventricular myocardial non-compaction were recognized at short axis view (*Figure 1H*). Right ventricular morphology, size, and systolic function were normal. To investigate cause and pathway of cardiomyopathy, after informed consent, the patient underwent cardiac catheterization with coronary and left ventricular (LV) angiography and endomyocardial biopsy (EMB). Coronary arteries were normal.

Materials and methods

Morphology (optical microscopy and transmission electron microscopy)

For optical microscopy (OM) EMB fragments were fixed in formalin and embedded in paraffin following standard procedures. For transmission electron microscopy (TEM) two EMB samples were fixed in glutaraldehyde and osmium tetroxide and embedded in an EPON-812 resin mixture. Ultrathin sections were double stained with lead hydroxide and a substitute of uranyl acetate and finally analysed with a JEOL 1400 Plus TEM.

Figure 1 Cardiac magnetic resonance imaging. Longitudinal (A) and horizontal (B) long axis on end-diastole demonstrated hypertrabeculated myocardium (black arrows) with slight increase of volume cavity. Left ventricular function was slightly decreased due to a mild hypokinesia of the apical segments and dissynergy of the latero-apical wall, as showed in end-systolic cineMR image (C). End-systolic cineMR images oriented on longitudinal (D) long axis and three chamber (E) views reveal a marked elongation of the mitral valve leaflets (in particular the anterior) associated with severe mitro-annular disjunction (black arrows) and regurgitation jet (white arrows). No areas of myocardial fibrosis have been detected on late gadolinium enhanced T1 weighted images (F). CineMR images acquired on short-axis (G).

Culture fibroblasts and adenosine triphosphate content

- *Cellular adenosine triphosphate (ATP) content* was assayed luminometrically in fibroblasts obtained from a cutaneous biopsy using the ATP-Lite 1 Step (PerkinElmer, Boston) according to the procedure recommended by the manufacturer. The fibroblasts (5×10^3) were cultivated either in a regular medium as well as in galactose supplemented medium (5 mM) for 24, 48, and 72 h. Luminescence was measured using the EnSpire Multimode Plate Readers (PerkinElmer).
- *Complex V activity* (in the direction of ATP synthesis) was measured in fibroblast mitochondria, with succinate, malate, or pyruvate + malate as substrates, and using reported spectrophotometric methods.[4] For all experiments aged matched controls have been used.

Statistical analysis

Data are presented as mean ± SD. The Student's *t* test was used for the analysis of statistical significance. A *P* value <0.05 was considered significant (**$P < 0.005$; ***$P < 0.0005$).

Genetic study

Analysis was undertaken by next-generation-sequencing (NGS) using the Illumina TruSight One (San Diego, CA, USA) sequencing panel of 4813 genes associated with human genetic diseases as previously reported.[5]

Results

Cardiac catheterization and angiography

LV end-diastolic pressure was elevated (18 mmHg) while coronary arteries were normal.

Morphology

At histology cardiomyocytes were hypertrophied and separated by large unendotheliolized interstitial spaces. Sometimes individual myocytes were completely disconnected from adjacent cells (*Figure 2A*).

The ultrastructure at TEM (*Figure 2B–F*) showed numerous cytoskeletal and mitochondrial abnormalities. Myocardiocytes appeared separated by large lateral intercellular spaces (*Figure 2A,C,E*) with rare or absent lateral adherents plaques; the intercalated discs were partially disorganized, as shown by lacunae of extracellular space located al level of cellular poles (*Figure 2B,C*); mitochondria were grouped in large clusters, mostly localized in the perinuclear space indicating some abnormality in the organelle movement, normally necessary for a regular distribution throughout the cytosol (*Figure 2D*).

In addition, mitochondria presented diffuse vacuolization of the matrix (*Figure 2E*) and, occasionally, fusion of adjacent membranes of the cristae (*Figure 2F*), and inhomogeneous matrix, suggesting a functional damage of this compartment. The altered function of mutated calreticulin, leading to an abnormal mitochondrial Ca^{2++} homeostasis, could be responsible for such damage, both structural and functional.

Genetic study

Next-generation-sequencing analysis identified in the proband a compound heterozygous genotype for two pathogenic variants (c.[4411 T > C];[6408 T > A], p[Ser1471Pro]; [Tyr2136Ter]) in the *MYO7* gene (MIM #276903), which encodes the MYO7 protein, a member of the myosin proteins, whose bi-allelic mutations cause US Type I. In addition, NGS analysis identified a heterozygous pathogenic variant (c.[702 + 2 T > G];[702 + 2=]) predicted to abolish the canonical donor splice site of the exon 5 of *CALR* gene, which encodes for calreticulin, an ubiquitous and major Ca^{2+} binding protein, resident mainly in the endoplasmic reticulum (ER) of eukaryotic cells, where it functions as a ER-membrane chaperone.

Mitochondrial metabolic function

To explore the effect of mutated calreticulin we studied the energy production by fibroblasts cultured from skin biopsy of our patient. The ATP content in whole fibroblasts was normal respect to controls in regular medium, but was significantly reduced in galactose medium, starting from 48 h treatment (*Figure 3A*). This reflects a lower efficiency of ATP production by OXPHOS in stress condition, as confirmed by the morphological changes described in myocardiocytes (*Figure 3E*).

Based on the above results, we performed indirect evaluation of the OXPHOS status in fibroblasts mitochondria by measuring the ATP synthesis, which showed a slight although significant reduction (~20–30%) with all substrates used (*Figure 3B*). In addition, the supplementation of galactose instead of glucose in the growing medium (the galactose forces the cell to use the mitochondria), displayed an additional 30% reduction on the synthesis of ATP (*Figure 3C*). Any variation in the ATP synthesis was evident in controls fibroblasts after galactose supplementation.

Figure 2 (A) Optical microscopy of endomyocardial biopsy sample. Cardiomyocytes are hypertrophied and separated by large interstitial spaces, as usually seen in non-compaction myocardium. The bar represents 15 μm. (B) At transmission electron microscopy, the intercalated discs are partially disorganized, as shown by lacunae of extracellular space located al level of cellular poles (arrows). The bar represents 2 μm. (C) Myocardiocytes are separated by large lateral intercellular spaces (arrows) with rare or absent lateral adherens plaques. The bar represents 1 μm. (D) Mitochondria are frequently grouped in large clusters, mostly localized in the perinuclear space, unlike the diffuse distribution seen in normal myocardium. This suggests an abnormality in the organelle movement throughout the cytosol due to the malfunction of (myosin 7A/γ-actin) contractile machinery. The bar represents 1 μm. (E) Mitochondria presented diffuse vacuolization with an inhomogeneous matrix, or a dilatation of intracristal spaces. Both suggest a functional damage of this compartment. The bar represents 0.4 μm. (F) Occasionally, mitochondrial cristae display fusion of adjacent membranes, as indicated by the electron-dense apposition marked by the arrows. The bar represents 0.6 μm.

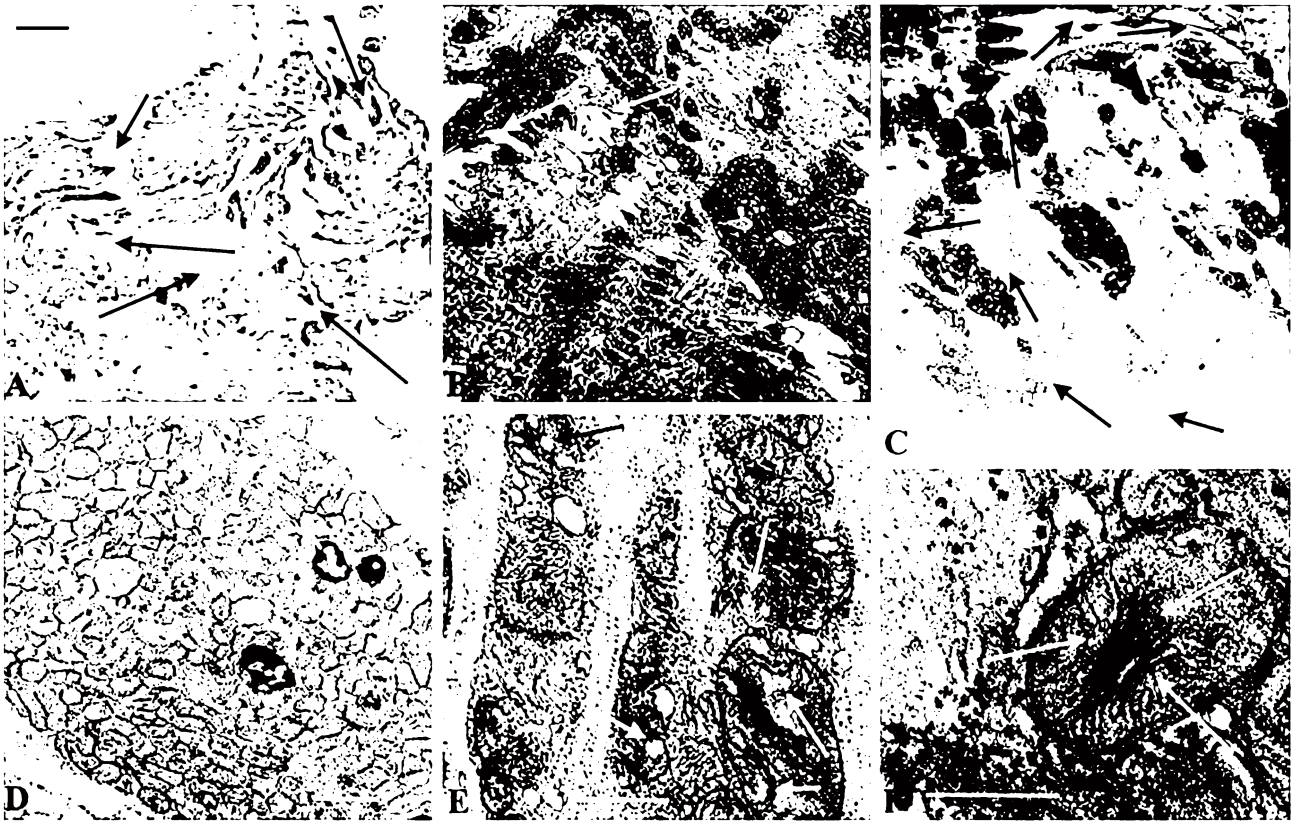

Treatment

The patient received carvedilol 25 mg bid and amiodarone 200 mg daily. At sequential clinical controls and Holter monitorings, LV dimension and function (EF 45%) remained stable while no recurrences of ventricular tachycardia were registered at 18 months follow up.

Discussion

A myocardial disease, to the best of our knowledge, has not been previously reported in association with Usher syndrome (US). In our study, it looks to be the result of concurring mutations involving *MYO7A* and *CALR* genes. They appear to alter two major compartments of myocardial composition: sites of cardiomyocyte connection and mitochondria. Consequences of the first alteration is cell disconnection and on clinical ground LV dilatation and dysfunction and ventricular tachyarrhythmias causing recurrent syncope. Mitral prolapse with annular disjunction and valve regurgitation, in the absence of redundant leaflets or elongated cords, appear to be related to hypotonia and dissynergy of papillary muscles secondary to myocyte hypocontractility and disconnection.

Structure and function of mitochondria are the other target of cardiomyopathy. Structurally, mitochondria appear grouped as result of intracellular non-muscle myofilament dysfunction, present vacuolar degeneration of the matrix and focal fusion of cristae membranes. These morphological changes are associated with reduction of 30% ATP production in patient cultured fibroblasts. It is likely that functional impact on cardiomyocytes provided of contractile activity and higher energy requirements might be more pronounced concurring to cardiac dilatation and dysfunction.

Figure 3 (A) Adenosine triphosphate (ATP) content assessed in controls (Ctrl) and patient fibroblasts cultured either in regular medium (RM) or in medium supplemented with galactose (GAL) for 24, 48, and 72 h. The ATP was moderately impaired starting at 48 h of treatment. Data are presented as a mean ± SD of at least four independent experiments run in triplicate; $^{**}P < 0.005$. (B) Spectrophotometric determination of complex V activity on fibroblast mitochondria of control (Ctrls) and patient growth in regular medium. The activity of complex V was reduced around 30% with all substrates used [succinate, or malate, or malate + pyruvate (pyr + mal)]. Data are presented as a mean ± SD of at least four independent experiments for the patient and 50 different experiments in 10 aged matched controls. (C) Spectrophotometric determination of complex V activity on patient mitochondria derived from fibroblasts growth in regular medium (RM) or in galactose supplemented medium (GAL) for 48 h. Either succinate, or malate, or malate + pyruvate (pyr + mal) were used as substrate. Data are presented as a mean ± SD of at least three independent experiments. $^{***}P < 0.0005$.

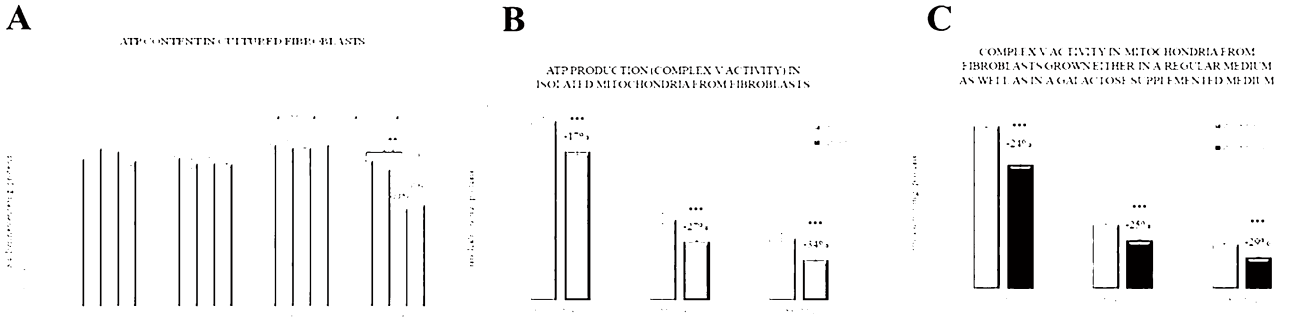

As far as molecular aspect is concerned, Myosin 7A is a member of non-conventional non sarcomeric myosins.[2] Together with non-muscle actin filaments, it provides the contractile machinery for a large number of cytoskeletal dynamics, such as cytokinesis, intracellular organellar movements, migration, maintenance of cell polarity and shape, mechano-electrical transduction, cell-to-cell adhesion, and cell-to-extracellular matrix interactions. In last two contexts, it contributes to the formation and function of tight junctions, desmosomes, hemi-desmosomes, or adhesion plaques, which are major components of intercalated disc in the myocardium.[2,6] Summarizing, in this patient, *MYO7A* mutation is likely to have a major role on myocyte disconnection and impaired function of intracellular myofilaments involved in cytoplasmic particle movement, including regular mitochondrial distribution.

CALR gene mutation may contribute to several aspects of mitochondrial disease and cell-to-cell contact. In particular, calreticulin is a Ca^{2+} binding protein, mainly localized in the smooth domain of ER and in the mitochondria.[7] Its main function is related to the Ca^{2+} homeostasis and its complex signalling, regulating a large number of important cell functions.

In particular, (i) it binds Ca^{2+}, contributing to the buffering cytosolic/cisternae of ER/mitochondrial pCa; (ii) it is part of the Ca^{2+} metabolic signalling; and (iii) it acts as chaperone for the correct folding of the nascent proteins from ER.

Confirmation of role of *CALR* gene mutation in the pathogenesis of dilated cardiomyopathy observed in our case, comes from animal studies. In particular, Zhang *et al*.[8] report in a rat model of dilated cardiomyopathy calreticulin-STAT3 signalling pathway to modulate mitochondrial function; Li *et al*.[9] document calreticulin gene mutation causing an impairment of myofibrillogenesis; Lee *et al*.,[10] reveal in a mouse model with up-regulation of calreticulin gene a reduced expression of gap junction proteins connexin 43 and 45. These last changes may explain the reduced cell-to-cell adhesion of cardiomyocytes that under prolonged contraction and wall stress may lead to myocyte separation.

On the other hand, cell disconnection is not a normal histologic finding of idiopathic dilated cardiomyopathy, and CMR features fail to identify the established diagnostic criteria for LV non-compaction cardiomyopathy.[11]

Summarizing combined mutation of *MYO7A* and *CALR* genes realizes a peculiar form of dilated cardiomyopathy that differs from idiopathic dilated cardiomyopathy as well as from LV non-compaction cardiomyopathy.

On therapeutic ground, the patient received benefit from combined administration of carvedilol and amiodarone with prevention of cardiac functional deterioration and recurrence of major (ventricular tachycardia) ventricular tachyarrhythmias and syncopal episodes.

In conclusion, US may include in its manifestations a peculiar form of dilated cardiomyopathy deriving from coincident mutation of *MYO7A* and *CALR* genes causing cardiomyocyte disconnection and mitochondrial dysfunction.

Conflict of interest

The authors declare no conflict of interest.

Funding

This work was supported by funding of the Italian Ministry of Health (*Ricerca corrente*) given to IRCCS Spallanzani and

IRCCS San Raffaele Pisana and by the European Project ERA-CVD 'Transnational Research Projects on Cardiovascular Diseases' (JTC 2016 IKDT-IGCM).

Supporting information

Additional supporting information may be found online in the Supporting Information section at the end of the article.

Movie S1. Video 1, 2: CineMR images acquired on horizontal and vertical long axes and three chamber views demonstrate a hypokinesis of LV apical segments and dissynergy of the latero-apical wall. An abnormal redundancy of the mitral valve leaflets, associated with moderate valve regurgitation and mitral annular disjunction, is well appreciated combined with excessive stretching of the tendon cords and hypocontraction of the posterior papillary muscle.

Movie S2. Video 1, 2: CineMR images acquired on horizontal and vertical long axes and three chamber views demonstrate a hypokinesis of LV apical segments and dissynergy of the latero-apical wall. An abnormal redundancy of the mitral valve leaflets, associated with moderate valve regurgitation and mitral annular disjunction, is well appreciated combined with excessive stretching of the tendon cords and hypocontraction of the posterior papillary muscle.

References

1. Boughman JA, Vernon M, Shave KA. Usher syndrome: definition and estimate of prevalence from two high-risk populations. *J Chronic Dis* 1983; **36**: 595–603.
2. Trivedi DV, Nag S, Spudich A, Ruppel KM, Spudich JA. The myosin family of mechanoenzymes: from mechanisms to therapeutic approaches. *Annu Rev Biochem* 2020; **89**: 667–693.
3. Van Waning JI, Caliskan K, Hoedemaekers YM, van Spaendonck-Zwarts KY, Baas AF, Boekholdt SM, van Melle JP, Teske AJ, Asselbergs FW, Backx APCM, du Marchie Sarvaas GJ, Dalinghaus M, Breur JMPJ, Linschoten MPM, Verlooij LA, Kardys I, Dooijes D, Lekanne Deprez RH, IJpma AS, van den Berg MP, Hofstra RMW, van Slegtenhorst MA, Jongbloed JDH, Majoor-Krakauer DJ. Genetics, clinical features and long term outcome of noncompaction cardiomyopathy. *Am Coll Cardiol* 2018; **71**: 711–722.
4. Rizza T, Vazquez-Memije ME, Meschini MC, Bianchi M, Tozzi G, Nesti C, Piemonte F, Bertini E, Santorelli FM, Carrozzo R. Assaying ATP synthesis in cultured cells: a valuable tool for the diagnosis of patients with mitochondrial disorders. *Biochem Biophys Res Commun* 2009; **383**: 58–62.
5. Ferese R, Bonetti M, Consoli F, Guida V, Sarkozy A, Lepri FR, Versacci P, Gambardella S, Calcagni G, Margiotti K, Piceci Sparascio F, Hozhabri H, Mazza T, Digilio MC, Dallapiccola B, Tartaglia M, Marino B, Hertog JD, De Luca A. Heterozygous missense mutations in NFATC1 are associated with atrioventricular septal defect. *Hum Mutat* 2018; **39**: 1428–1441.
6. Muller M, Diensthuber RP, Chizhov I, Claus P, Heissler SM, Preller M, Taft MH, Manstein DJ. Distinct functional interactions between actin isoforms and non-sarcomeric myosins. *PLoS One* 2013; **8**: e70636.
7. Zhang M, Wei J, Li Y, Hu S, Yan R, Lin L, Zhang Q, Xue J. Novel distribution of calreticulin to cardiomyocyte mitochondria and its increase in a rat model of dilated cardiomyopathy. *BiochemBiophys Res Commun* 2014; **449**: 62–68.
8. Zhang M, Wei J, Shan H, Wang H, Zhu Y, Xue J, Lin L, Yan R. Calreticulin-STAT3 signaling pathway modulates mitochondrial function in a rat model of furazolidone-induced dilated cardiomyopathy. *PLoS One* 2013; **8**: e66779.
9. Li J, Pucéat M, Perez-Terzic C, Mery A, Nakamura K, Michalak M, Krause K-H, Jaconi ME. Calreticulin reveals a critical Ca^{2+} checkpoint in cardiac myofibrillogenesis. *J Cell Biol* 2002; **158**: 103–113.
10. Lee D, Oka T, Hunter B, Robinson A, Papp S, Nakamura K, Srisakuldee W, Nickel BE, Light PE, Dyck JRB, Lopaschuk GD, Kardami E, Opas M, Michalak M. Calreticulin induces dilated cardiomyopathy. *PLoS One* 2013; **8**: e56387.
11. Weir-McCall JR, Yeap PM, Papagiorcopulo C, Fitzgerald K, Gandy SJ, Lambert M, Belch JJF, Cavin I, Littleford R, Macfarlane JA, Matthew SZ, Nicholas RS, Struthers AD, Sullivan F, Waugh SA, White RD, Houston JG. Left ventricular noncompaction: anatomical phenotype or distinct cardiomyopathy? *J Am Coll Cardiol* 2016; **68**: 2157–2165.